Electrical Engineering (2022) 104:3685–3695
https://doi.org/10.1007/s00202-022-01578-5

ORIGINAL PAPER

Sensorless sliding mode control method for a three-phase induction motor

Nguyen Vinh Quan[1] · Mai Thang Long[2]

Received: 20 January 2022 / Accepted: 5 May 2022 / Published online: 27 May 2022

Abstract
This paper improved a sensorless sliding mode control strategy for the three-phase induction motor system. Based on the decoupled control scheme, two sliding mode controllers for the flux and rotor speed are the main control method for the tracking control. In the proposed sliding mode strategy, the sliding mode surfaces as the nonlinear exponential function are applied to reduce the chattering phenomena. The requirement of the rotor speed is relaxed by the observer based neural networks estimator. In addition, the online updating algorithm for the speed observer and the SMC control laws are obtained in the sense of the Lyapunov stability theorem. Therefore, the stability, robustness and tracking control features are guaranteed. The effectiveness of the proposed control system is demonstrated by comparative simulation and experiment results for the three-phase asynchronous induction motor 1 hp.

Keywords Induction motor · Sliding mode control · Sensorless control · Neural network

List of symbols

R_s, R_r	Stator, rotor resistances
L_s, L_r, L_m	Stator, rotor, mutual inductance
u_{sq}, u_{sd}	Stator voltages (d–q axis)
u_{rq}, u_{rd}	Rotor voltages (d–q axis)
i_{sq}, i_{sd}	Stator currents (d–q axis
i_{rq}, i_{rd}	Rotor currents (d–q axis)
φ_{sq}, φ_{sd}	Stator fluxes (d–q axis)
φ_{rq}, φ_{rd}	Rotor fluxes (d–q axis)
ω_r	Angular velocity
T_e, T_m	Electromagnetic, load torque
p	Pole-pairs
B	Friction coefficient
J	Inertia constant

✉ Mai Thang Long
maithanglong@iuh.edu.vn

Nguyen Vinh Quan
quannv@hcmute.edu.vn

[1] Faculty of Electrical and Electronics Engineering, HCMC University of Technology and Education, Ho Chi Minh City, Vietnam

[2] Faculty of Electronics Technology, Industrial University of Ho Chi Minh City, Ho Chi Minh City, Vietnam

1 Introduction

In industrial applications, nowadays, the three phase induction motor (TIM) is one of the most electric machines that is largely applied, due its robustness and efficiency. Therefore, the research on control system in order to improve the effectiveness of the TIM applications always attracts many attentions from researchers in the world [1–7]. However, the model of the TIM is a fully complex nonlinear system, with multiple inputs and outputs, the control for TIM is not easy to implement, especially in real applications. As well known, with the results in previous works [1–7], the vector-oriented control (VOC) method plays an important role in the design of control algorithms. For the TIM control, the VOC technique is a basic derivative to implement the decoupled control of d–q currents [2, 4, 5]. Based on this decoupled control, the sliding mode control (SMC) technique, with its advantages [8–10] as the stability and robustness features in the presence of time-varying disturbances, can be considered as the most popular control strategy for the TIM that is applied to be able to achieve high performance [11–22]. The authors in [11] combined a backstepping technique into the SMC method to position control for a linear induction motor. In this proposed method [11], to decrease the chattering phenomena, the signum function for the sliding switching surface is replaced by the saturated function. Clearly, in the SMC

methods for the TIM control, the chattering phenomena are the important problem that must be solved carefully in order to guarantee the robustness for the SMC control systems [9, 10]. For the TIM control system based the SMC, the chattering phenomena will be increased cause by fast and large amplitude variation of the TIM currents and voltages. Thus, the robustness and stability of the SMC system depend on the selection of the sliding and switching surfaces. To relax these problems for the electric machine SMC-control, Zhang et al. [19] proposed the reaching law (the switching surface) as a nonlinear exponential function. This reaching law can help the proposed control system [19] adapt to the variations of the switching surface and system states [18], suppress the chattering and discontinuous states (for using the signum function as the switching surface). In the other hand, the authors in [20] presented successfully the fast terminal sliding mode scheme to deal with chattering phenomena and improve the control performance for the motor-SMC system. Thus, we can realize that the SMC systems using the sliding nonlinear functions can achieve better the chattering-reducing performances than those of the sliding linear functions [19–22].

Accordance with the improving of the control effectiveness, research on the position sensorless control for the electric machines have been explored strongly in recent years [23–32]. Wang et al. in [25] implemented quite well a back electromotive force detection method as a sensorless control for the motor for the high order SMC control without Hall sensors. Based on the previous research works [23–32], we easy see that observer systems-based approaches can be considered as a useful scheme for the TIM sensorless control methods. By applying, the observers-based models [23–25, 27, 30–32], these approaches achieved good performances for the TIM control systems. However, because highly dependent on the measured signals of the electric machine control systems, the complexity of system design and numerical calculations will have to increase. In the different approach, the results in [26, 28, 29] proposed the observer based on the soft computing techniques for the TIM sensorless control. These proposed observer [26, 28, 29], have proved the effectiveness of the TIM sensorless control systems in reducing the disadvantages of the observer systems-based models that are the complexity of the control systems and computation burden.

In this research, by applying the merits of the SMC sensorless control methods based soft computing techniques, the decoupled SMC system will be proposed without the requirement of the TIM speed information. The first, the decoupled control method as the VOC technique will create two independent controllers for the flux and rotor speed based the SMC scheme. In order to reduce the chattering phenomena, in the proposed SMC controllers, the sliding mode surface is applied as the nonlinear function that is the hyperbolic tangent sigmoid function (tansig function). The second, the rotor speed of the TIM system will be online estimated by using an observer based the radial basic function (RBF) neural networks (NN). Moreover, the online NN updating algorithm and the SMC laws are designed by using the Lyapunov stability theorem such that the stability and adaptability of the proposed SMC sensorless control system for the TIM are guaranteed.

The paper is organized as follows. Section II describes the dynamics model of the TIM and the problem formulation for the SMC decoupled control strategies. In Section III, the SMC sensorless control algorithms are presented. The comparative simulation and experimental results for the TIM control system are included in Section IV. Finally, conclusion is drawn in Section V.

2 Preliminaries

2.1 System description

We will consider the nonlinear model of the three-phase asynchronous induction motor in the d–q stationary reference frame as the following vector–matrix form [33]:

The stator and rotor voltage equations:

$$\begin{bmatrix} u_{sd} \\ u_{sq} \end{bmatrix} = \begin{bmatrix} R_s & 0 \\ 0 & R_s \end{bmatrix} \begin{bmatrix} i_{sd} \\ i_{sq} \end{bmatrix} + \frac{d}{dt} \begin{bmatrix} \varphi_{sd} \\ \varphi_{sq} \end{bmatrix} + \begin{bmatrix} 0 & -\omega_e \\ \omega_e & 0 \end{bmatrix} \begin{bmatrix} \varphi_{sd} \\ \varphi_{sq} \end{bmatrix} \tag{1}$$

$$\begin{bmatrix} 0 \\ 0 \end{bmatrix} = \begin{bmatrix} R_r & 0 \\ 0 & R_r \end{bmatrix} \begin{bmatrix} i_{rd} \\ i_{rq} \end{bmatrix} + \frac{\mathrm{d}}{\mathrm{d}t} \begin{bmatrix} \varphi_{rd} \\ \varphi_{rq} \end{bmatrix} + \begin{bmatrix} 0 & -(\omega_e - p\omega_r) \\ (\omega_e - p\omega_r) & 0 \end{bmatrix} \begin{bmatrix} \varphi_{rd} \\ \varphi_{rq} \end{bmatrix} \tag{2}$$

The stator and rotor flux equations:

$$\begin{bmatrix} \varphi_{sd} \\ \varphi_{sq} \end{bmatrix} = \begin{bmatrix} L_s & 0 \\ 0 & L_s \end{bmatrix} \begin{bmatrix} i_{sd} \\ i_{sq} \end{bmatrix} + \begin{bmatrix} L_m & 0 \\ 0 & L_m \end{bmatrix} \begin{bmatrix} i_{rd} \\ i_{rq} \end{bmatrix} \tag{3}$$

$$\begin{bmatrix} \varphi_{rd} \\ \varphi_{rq} \end{bmatrix} = \begin{bmatrix} L_m & 0 \\ 0 & L_m \end{bmatrix} \begin{bmatrix} i_{sd} \\ i_{sq} \end{bmatrix} + \begin{bmatrix} L_r & 0 \\ 0 & L_r \end{bmatrix} \begin{bmatrix} i_{rd} \\ i_{rq} \end{bmatrix} \tag{4}$$

The torque equations:

$$\begin{cases} T_e = \frac{3}{2} p \begin{bmatrix} \varphi_{sd} & \varphi_{sq} \end{bmatrix} \begin{bmatrix} i_{sq} \\ -i_{sd} \end{bmatrix} \\ J \frac{\mathrm{d}}{\mathrm{d}t} \omega_r = (T_e - B\omega_r - T_m) \end{cases} \tag{5}$$

We note that, if the d-axis of the reference frame is aligned with the stator flux vector [33], we have the following results:

$$\varphi_{sq} = \dot{\varphi}_{sq} = 0 \tag{6}$$

$$u_{sq} = R_s i_{sq} + \omega_r \varphi_{sd} \tag{7}$$

$$u_{sd} = R_s i_{sd} + \dot{\varphi}_{sd} \tag{8}$$

$$T_e = \frac{3}{2} p(\varphi_{sd} i_{sq}) \tag{9}$$

$$\varphi_{sd} = \int (u_{sd} - R_s i_{sd}) \mathrm{d}t \tag{10}$$

In this paper, the SMC based on the decoupled VOC method will be consider for the control of the stator flux and the rotor speed. The characteristics of the proposed SMC controllers will be analyzed as follows.

2.2 Stator flux control

In this study, we will apply the SMC technique to control the stator flux. Define the stator flux control error as:

$$e_F = \varphi_{sd}^* - \varphi_{sd} \tag{11}$$

where φ_{sd}^* is the desired stator flux that is bounded and uniformly continuous, and it also has derivative up to the second order. The sliding function for this control is defined as the following form:

$$S_F = c_1 e_F + \dot{e}_F \tag{12}$$

where c_1 is positive constant. Taking the derivative of S_F with respect to time and applying Eq. (8), yields:

$$\dot{S}_F = -c_1(u_{sd} - R_s i_{sd}) + c_1 \varphi_{sd}^* + \ddot{e}_F \tag{13}$$

In order to guarantee the stator flux control, the switching surface function (13) can be chosen as:

$$\dot{S}_F = -\varepsilon_F \mathrm{sign}(S_F) \tag{14}$$

where $\varepsilon_F > 0$, the $\mathrm{sign}(S_F)$ function is defined as:

$$\mathrm{sign}(S_F) = \begin{cases} 1, & S_F > 0 \\ 0, & S_F = 0 \\ -1 & S_F < 0 \end{cases} \tag{15}$$

Based on the SMC theory [9], from (13) and (14), the SMC input for the stator flux control can be determined as the following form:

$$u_{sd} = \frac{1}{c_1}(\varepsilon_F \mathrm{sign}(S_F) + \ddot{e}_F) + \dot{\varphi}_{sd}^* + R_s i_{sd} \tag{16}$$

Individually, this SMC input can be able to guarantee for the tracking control of the stator flux control. However, in the TIM control system, the effectiveness, robustness, and stability of the stator flux control are dependent heavily on the control of the rotor speed performance. In addition, the SMC always has the inevitable chattering phenomena with the signum $\mathrm{sign}(S_F)$ switching function.

2.3 Rotor speed control

Similar to the stator flux control, the SMC method will be applied to control the rotor speed. Define the rotor speed error as:

$$e_M = \omega_r^* - \omega_r \tag{17}$$

where ω_r^* is the desired rotor speed that is bounded and uniformly continuous, and it also has derivative up to the second order. The sliding function is defined as the following form:

$$S_M = c_2 e_M \tag{18}$$

where c_2 is positive constant By selecting the switching function as the same of the SMC for the stator flux control as:

$$\dot{S}_M = -\varepsilon_M \mathrm{sign}(S_M) \tag{19}$$

where $\varepsilon_M > 0$. And based on the SMC theory [9], in order to guarantee for the rotor speed tracking control, from (7), (10) and (19), with assumption that the good performance of the stator flux control can be obtained, the SMC control input can be designed as the following form:

$$\begin{aligned} u_M &= \int \dot{u}_{sq} \mathrm{d}t \\ &= \int \left(\omega_r \dot{\varphi}_{sd} + R_s \dot{i}_{sq} + \omega_r^* \varphi_{sd} + \frac{\varphi_{sd}}{c_2} \varepsilon_M \mathrm{sign}(S_F) \right) \mathrm{d}t \end{aligned} \tag{20}$$

However, with this SMC input for the rotor speed control, besides the inevitable chattering phenomena, this controller is only well done when the rotor speed ω_r can be measured.

In this practical research, the SMC without requirement of rotor speed information will be explored carefully. In the proposed controllers, the chattering phenomena are also relaxed in considering of control system stability. The proposed methods are analyzed and designed as follows.

3 Control algorithms

As we knew, the control goal was to improve the SMC methods for the stator flux and rotor speed tracking control of the TIM system as, $\varphi_s(t) \rightarrow \varphi_{sd}^*(t)$ and $\omega_r(t) \rightarrow \omega_r^*(t)$ as the

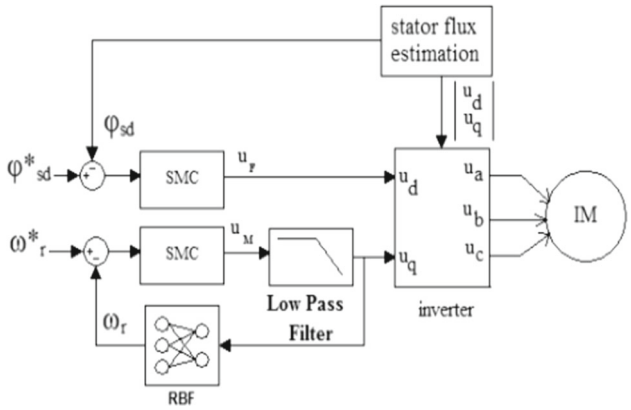

Fig. 1 The proposed control system strategy

time tends to infinite $t \to \infty$. The proposed control system strategy is drawn in Fig. 1.

Assumption 3.1 The φ^*_{sd} and ω^*_r are bounded and uniformly continuous.

Assumption 3.2 The ω_r signal cannot be measured by sensors.

3.1 SMC for the stator flux

As the aforementioned analysis for the stator flux control, the SMC controller has an inevitable drawback when the switching surface is the sign(S_F) signum function. The sign(S_F) is a linear function is used to smooth nonlinear discontinuous control. Therefore, the chattering phenomenon is likely to occur all the time, especially in cases the control system operates at high frequencies. In this study, in order to deal with this problem, we will apply the tansig(S_F) function to replace the sign(S_F) function. The tansig(S_F) is defined as the following form:

$$\text{tansig}(S_F) = \frac{2}{(1+e^{-2S_F})} - 1 \tag{21}$$

Clearly, the tansig(S_F) is a smooth nonlinear function, as shown in Fig. 2, it also is the exponential function with rapidly response. Thus, the chattering phenomenon around sliding surface can be decreased when the switching function use this tansig(S_F) function [19–22]. Based on this recommendation, from (21), the proposed SMC input for the stator flux control is designed as:

$$u_{sd} = \frac{1}{c_1}(\varepsilon_F \tan\text{sig}(S_F) + \ddot{e}_F + K_F s) + \dot{\varphi}^*_{sd} + R_s i_{sd} \tag{22}$$

where K_F is the positive constant.

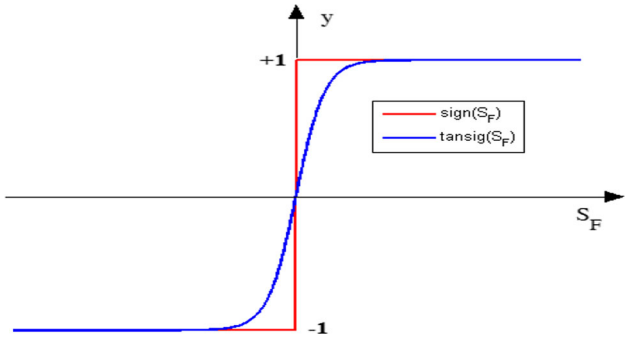

Fig. 2 The Tansig function response

3.2 SMC for the rotor speed

As shown in Fig. 1, the proposed SMC method for the rotor speed has some improvements so that to decrease the chattering phenomenon, relax the requirement of the rotor speed measurement and increase the time-response of control signal. The detailed design steps of the proposed SMC scheme for the rotor speed are presented clearly as follows.

The first, based on the SMC input for the rotor speed (20) that is considered as an integral control input, we will add a low-pass filter [34] to create the true control input for the rotor speed control. Therefore, we have the following relationship as:

$$u_{sd} = \frac{1}{\tau s + 1} u_M \tag{23}$$

where τ is an integral time constant, s is the Laplace operator, and, the following result can be obtained as:

$$u_M = u_{sd} + \tau \dot{u}_{sd} \tag{24}$$

By substituting the result in (7) into (24), we have:

$$\dot{\omega}_r = \frac{1}{\tau \varphi_{sd}}\left(u_M - R_s i_{sq} - \omega_r(\varphi_{sd} + \tau\dot{\varphi}_{sd}) - \tau R_s \dot{i}_{sq}\right) \tag{25}$$

From (18) and (25), the sliding switching function of the rotor speed control can be described as the following form:

$$\dot{S}_M = c_2\left(\dot{\omega}^*_r - \frac{1}{\tau\varphi_{sd}}\left(u_M - R_s i_{sq} - \omega_r(\varphi_{sd} + \tau\dot{\varphi}_{sd}) - \tau R_s \dot{i}_{sq}\right)\right) \tag{26}$$

here if the sliding switching function in (26) is the tansig(S_M) function for chattering phenomenon elimination, the SMC input for the rotor speed control can be designed as:

$$u_M = \tau\varphi_{sd}\dot{\omega}^*_r + R_s i_{sq} + \omega_r(\varphi_{sd} + \tau\dot{\varphi}_{sd})$$

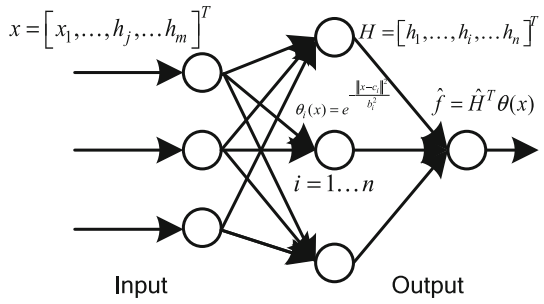

Fig. 3 The RBF NN structure

$$+ \tau R_s \dot{i}_{sq} + \frac{\tau \varphi_{sd}}{c_2}(\varepsilon_M \tan \text{sig}(S_M) + K_M S_M) \tag{27}$$

where K_M is the positive constant. However, follow to the Assumption 3.2, we have no knowledge of the rotor speed ω_r. Therefore, the SMC control input for the rotor speed control is modified as the following form:

$$u_M = \tau \varphi_{sd} \dot{\omega}_r^* + R_s i_{sq} + \hat{f}(\varphi_{sd} + \tau \dot{\varphi}_{sd}) + \tau R_s \dot{i}_{sq} + \frac{\tau \varphi_{sd}}{c_2}(\varepsilon_M \tan \text{sig}(S_M) + K_M S_M) \tag{28}$$

where the $\hat{f}$ is the estimator value of the $f = \omega_r$.

In the SMC method for the rotor speed control, the RBF NN as the observer system, will be applied to approximate the f function. And from this approximating value, the rotor speed value can be obtained. For simplicity, the NN estimator structure has one hidden layer with activation function is the Gaussian function [35], as shown in Fig. 3. The NN output can be denoted as:

$$f = H^T \theta(x) \tag{29}$$

where $H = [h_1, \ldots, h_i, \ldots h_n]^T$, $i = 1 \ldots n$, h_i is the weight between the hidden layer and the output layer, n is the number of hidden nodes. $x = [x_1, \ldots, h_j, \ldots h_m]^T$, $j = 1 \ldots m$ is the number of inputs. The $\theta(x) = [\theta_1, \ldots, \theta_i, \ldots, \theta_n]^T$, θ_i is the Gaussian function:

$$\theta_i(x) = e^{-\frac{\|x-c_i\|^2}{b_i^2}} \tag{30}$$

where $c_i = [c_{1i}, \ldots, c_{ji}, \ldots, c_{mi}]^T$ is the coordinate value of center point of the Gaussian function, $b_i = [b_{1i}, \ldots, b_{ji}, \ldots, b_{mi}]^T$ is the width value of the Gaussian function. Based on the universal approximation analysis [35], an ideal NN structure with its optimal parameters has following form as:

$$f = H^{*T} \theta(x) \tag{31}$$

where H^* is the unknown optimal value. And from (28) and (31), the NN estimator output can be described as:

$$\hat{f} = \hat{H}^T \theta(x) \tag{32}$$

where $\hat{H}$ is the approximating value of the H^*.

By defining $\tilde{f} = f - \hat{f}$, $\tilde{H} = H^* - \hat{H}$, follow to (25, 28, 31, 32), and assuming that we can obtain the following result as:

$$\begin{aligned} \dot{S}_M &= \frac{c_2}{\tau \varphi_{sd}}(\varphi_{sd} + \tau \dot{\varphi}_{sd})\tilde{f} - \varepsilon_M \tan \text{sig}(S_M) - K_M S_{ds} \\ &= \frac{c_2}{\tau \varphi_{sd}}(\varphi_{sd} + \tau \dot{\varphi}_{sd})\tilde{H}^T \theta \\ &\quad - \varepsilon_M \tan \text{sig}(S_M) - K_M S_M \end{aligned} \tag{33}$$

Based on the Lyapunov stability theorem [36], the adaptive online learning algorithm for the RBF NN is proposed as:

$$\dot{\hat{H}} = K_H \frac{c_2}{\tau \varphi_{sd}}(\varphi_{sd} + \tau \dot{\varphi}_{sd}) \theta S_M \tag{34}$$

where K_H is the positive and diagonal constant matrix.

3.3 Stability analysis

Theorem By considering that the TIM dynamics in the Eqs. (1–10), all Assumptions hold. If the SMC law for the stator flux control is designed as (22), the SMC law for the rotor speed control and the online updating algorithm for the RBF NN estimator are designed as (28) and (34), then,

(1) The S_F converges to zero.
(2) The e_M converges to zero and the RBF NN weights are bounded. The stability of the proposed TAIM control system is guaranteed.

Proof (1) For the stator flux control, we consider the Lyapunov candidate function as the following form:

$$V_1(S_F(t)) = \frac{1}{2} S_F^2 \tag{35}$$

By differentiating (35) with respect to time, we have:

$$\dot{V}_1 = S_F \dot{S}_F \tag{36}$$

By substituting (13) into (36), it yields:

$$\dot{V}_1 = S_F(-c_1(u_{sd} - R_s i_{sd}) + c_1 \varphi_{sd}^* + \ddot{e}_F) \tag{37}$$

If the SMC law for the stator flux control is chosen as (22), then, (37) can be described as:

$$\dot{V}_1 = -\varepsilon_F S_F \tan \text{sig}(S_F) - K_F S_F^2$$

$$\leq - K_F S_F^2 \tag{38}$$

Clearly, $\dot{V}_1 \leq 0$, and based the Lyapunov theorem [36], from this results, we easy to conclude that the stability of the SMC system for stator flux control is guaranteed and S_F will converge to zero as time tends to infinite. Therefore, the stator flux control is guaranteed.

Proof (2) For the rotor speed control, we consider the Lyapunov candidate function as the following form:

$$V_2(S_M(t),\ \tilde{H}) = \frac{1}{2}S_M^2 + \frac{1}{2}\tilde{H}^T K_H^{-1}\tilde{H} \tag{39}$$

By differentiating (39) with respect to time, it yields:

$$\begin{aligned}\dot{V}_2 &= S_M \dot{S}_M + \tilde{H}^T K_H^{-1}\dot{\tilde{H}} \\ &= S_M \dot{S}_M - \tilde{H}^T K_H^{-1}\dot{\hat{H}}\end{aligned} \tag{40}$$

By substituting (33) into (40), one can obtain:

$$\begin{aligned}\dot{V}_2 &= S_M\Big(\frac{c_2}{\tau\varphi_{\mathrm{sd}}}(\varphi_{\mathrm{sd}} + \tau\dot{\varphi}_{\mathrm{sd}})\tilde{H}^T\theta - \varepsilon_{\mathrm{M}}\tan\mathrm{sig}(S_{\mathrm{M}}) \\ &\quad - K_{\mathrm{M}}S_{\mathrm{M}}\Big) - \tilde{H}^T K_{\mathrm{H}}^{-1}\dot{\hat{H}} \\ &= -\varepsilon_{\mathrm{M}}S_{\mathrm{M}}\tan sig(S_{\mathrm{M}}) - K_{\mathrm{M}}S_{\mathrm{M}}^2 \\ &\quad + \frac{c_2}{\tau\varphi_{\mathrm{sd}}}(\varphi_{\mathrm{sd}} + \tau\dot{\varphi}_{\mathrm{sd}})\tilde{H}^T\theta S_{\mathrm{M}} - \tilde{H}^T K_{\mathrm{H}}^{-1}\dot{\hat{H}}\end{aligned} \tag{41}$$

If the adaptive algorithm of the NN estimator for rotor speed is chosen as (34), it is concluded that:

$$\begin{aligned}\dot{V}_2 &= -\varepsilon_{\mathrm{M}}S_{\mathrm{M}}\mathrm{tansig}(S_{\mathrm{M}}) \\ &\quad - K_{\mathrm{M}}S_{\mathrm{M}}^2 + \frac{c_2}{\tau\varphi_{\mathrm{sd}}}(\varphi_{\mathrm{sd}} + \tau\dot{\varphi}_{\mathrm{sd}})\tilde{H}^T\theta S_{\mathrm{M}} \\ &\quad - \tilde{H}^T K_H^{-1}(K_H\frac{c_2}{\tau\varphi_{\mathrm{sd}}}(\varphi_{\mathrm{sd}} + \tau\dot{\varphi}_{\mathrm{sd}})\theta S_M) \\ &= -\varepsilon_{\mathrm{M}}S_{\mathrm{M}}\mathrm{tansig}(S_{\mathrm{M}}) - K_{\mathrm{M}}S_{\mathrm{M}}^2 \leq -K_{\mathrm{M}}S_E^2\end{aligned} \tag{42}$$

Based on the result in (42), $\dot{V}_2(S_M(t),\ \tilde{H})$ is a negative semi-definite function, $V_2(S_M(t),\ \tilde{H}) \leq V_2(S_M(0),\ \tilde{H})$. Clearly, if $S_M(t)$, $\tilde{H}$ are bounded at the time $t = 0$, then they will stay at this bounded state as $t \geq 0$. Therefore, the $S_M(t)$, $\tilde{H}$ are also bounded for $t \geq 0$. This conclusion is right for the $S_F(t)$ in the Proof (1).

Next, we consider the following definition: $\Xi(t) \equiv -K_M S_M^2$, and from (42), we have: $-\dot{V}_2 \geq \Xi(t)$, by integrating $\Xi(t)$ with respect to time, we will obtain the following result:

$$\int_0^t \Xi(\vartheta)d\vartheta \leq V_2(S_M(0),\ \tilde{H}) - V_2(S_M(t),\ \tilde{H}) \tag{43}$$

From the result as (43), based on above analysis, the $V_2(S_M(0),\ \tilde{H})$ is a bounded function, the $V_2(S_M(t),\ \tilde{H})$ also is a bounded non-increasing function, the following result can be achieved:

$$\lim_{t\to\infty}\int_0^t \Xi(\vartheta)d\vartheta < \infty \tag{44}$$

Thus, by applying the Barbalat's Lemma [36] with $\dot{\Xi}(t)$ is bounded, it shows that $\lim_{t\to\infty}\int_0^t \Xi(\vartheta)d\vartheta = 0$, and as a result, the $S_M(t)$ will converge to zero as time tends to infinite. As the result, from (18), we can conclude that the e_M also converges to zero as time tends to infinite.

Based the aforementioned results in Proof (1) and Proof (2), the stability and robustness of the proposed SMC controllers, for the stator flux and rotor speed, are guaranteed with all signals in the control system are bounded. The tracking errors of the stator flux and rotor speed will converge to zero as time tends to infinite.

Remark According to the analysis and designing of the proposed SMC controllers for the stator flux and rotor speed control, the requirement of the rotor speed measurement is relaxed. In addition, the NN estimator for the rotor speed estimation is designed with the online updating algorithm. This advantage has guaranteed the strictly state passive for the proposed control system based on the NN [35], improve the robustness and boundedness features. Moreover, in the SMC controller for the rotor speed control, we can also consider the stator flux is the constant parameter. If the assumption is hold, the control input (28) can be modified as:

$$\begin{aligned}u_{\mathrm{M}} =& \tau\varphi_{\mathrm{sd}}\dot{\omega}_{\mathrm{r}}^* + R_s i_{\mathrm{sq}} + \hat{f}(\varphi_{\mathrm{sd}}) + \tau R_s\dot{i}_{\mathrm{sq}} \\ &+ \frac{\tau\varphi_{\mathrm{sd}}}{c_2}(\varepsilon_{\mathrm{M}}\tan\mathrm{sig}(S_{\mathrm{M}}) + K_{\mathrm{M}}S_{\mathrm{M}})\end{aligned} \tag{45}$$

And the online updating algorithm (34) can be represented as the following form:

$$\dot{\hat{H}} = K_H\frac{c_2}{\tau}\theta S_M \tag{46}$$

The effectiveness for the tracking control and robustness of the proposed SMC controllers will be addressed by the following numerical and experimental results.

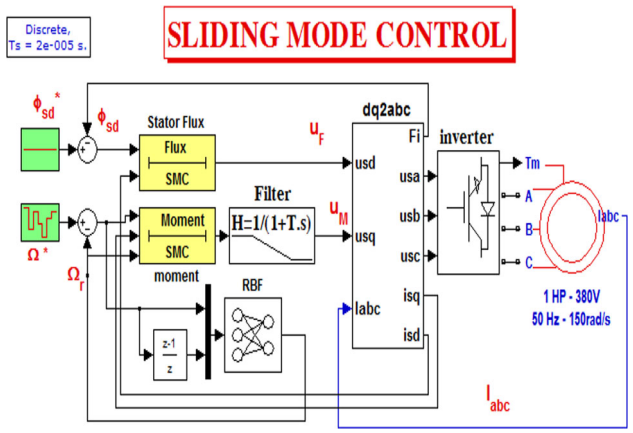

Fig. 4 The simulation diagram

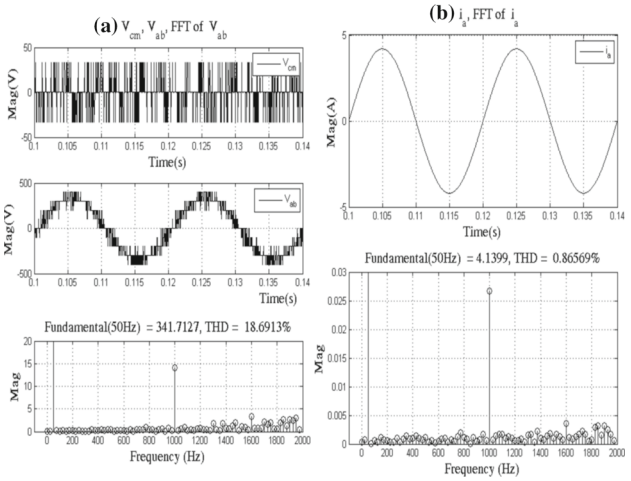

Fig. 5 The output responses of the three-phase 5-level cascaded inverters. **a** CMV, line voltage and FFT of line voltage, **b** phase current and FFT of phase current

Table 1 The TIM model parameters

Name	Value
Power	1 HP, 50 Hz
Votage (line–line)	380 V
w_r	150 rad/s
T_m	1 N.m
R_s, L_s	2.5 Ω, 5 mH
R_r, L_r	0.816 Ω, 5 mH
p	2
J	0.005 kg m^2
L_m	50.31 mH
T_s	20 μs

4 Simulation and experimental results

4.1 Simulation results

In order to verify the effectiveness of the proposed SMC methods, we shall consider the simulation model of the proposed control system that is shown in Fig. 4. The simulation process carried out using the Matlab-Simulink package with sample time is $T_s = 2.10^{-5}(s)$. The parameters of the TIM model are given as Table 1.

For first simulation case, by observing the results in Fig. 5, we can see the output responses of the three-phase 5-level cascaded inverter that are the common mode voltage (CMV), line voltage, phase current, and fast Fourier transform (FFT) of the phase current and line voltage. Based on the desired constant values of stator flux and rotor speed as $\varphi_{sd}^* = 1(\text{Wb})$, $\omega_r^* = 150(\text{rad/s})$, the CMV and THD of line voltage are $V_{cm} = V_{dc}/3$, $\text{THD}_V = 18.69(\%)$, the phase current and THD of phase current is $I_a = 4(A)$, $\text{THD}_I = 0.865(\%)$. In Fig. 6, the SMC controllers based on the NN has well guaranteed the tracking control for the stator flux and the rotor

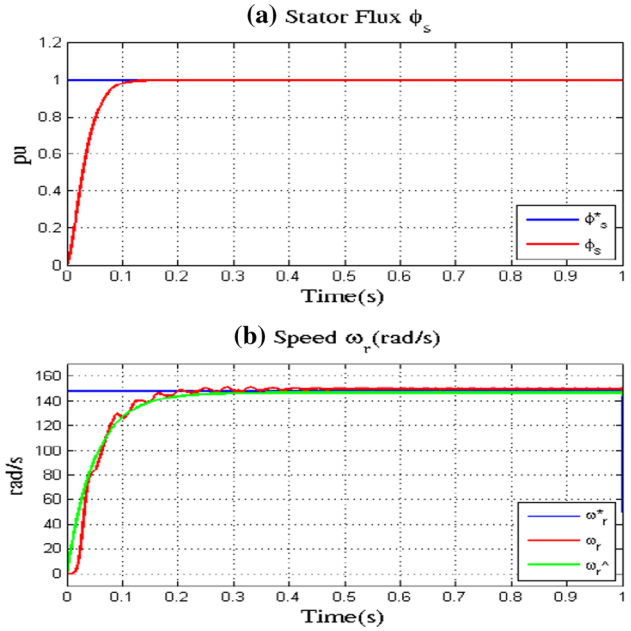

Fig. 6 The stator flux and rotor speed responses. **a** The stator flux, **b** the rotor speed

speed, with steady time are about 0.15 (s) and 0.25 (s) for the stator flux and the rotor speed, respectively. In addition, based on the result in Fig. 6b, the NN estimator also has good performance when it provides the rotor speed estimating value with good tracking performance in comparing to rotor speed measurement.

In the second simulation case, the desired rotor speed values are changed with respect to time (as shown on Fig. 7b). The simulation results for this case are provided in Fig. 7. Based on these results, we can draw the following comments. The SMC controllers based on the NN estimator for stator

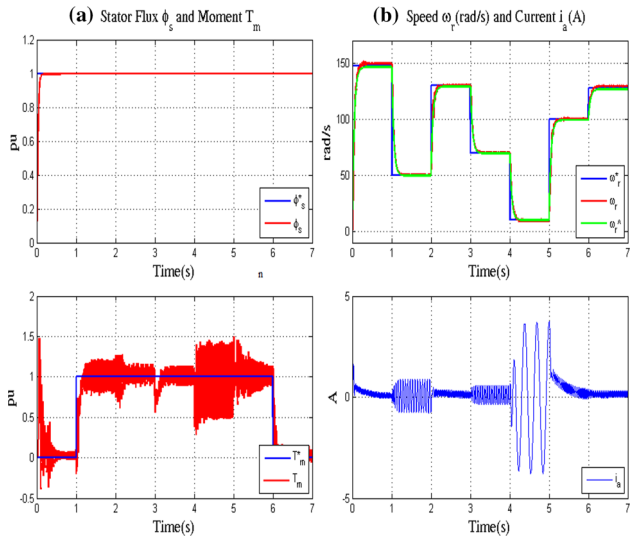

Fig. 7 The simulation results with case of changing the rotor speed. **a** The stator flux and torque T_{m}, **b** The rotor speed and phase current

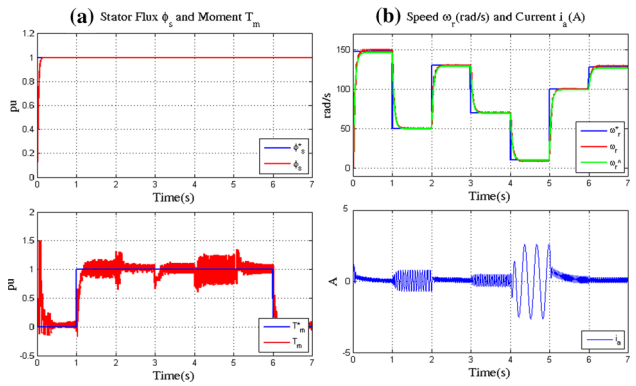

Fig. 8 The simulation results with case of changing the rotor speed and R_{s} is increased to 1.5 times. **a** The stator flux and torque T_{m}, **b** the rotor speed and phase current

flux and rotor speed still operate well with the changing of the desired rotor speed. In Fig. 7a, the torque of the TIM has occurred overshoot and strong vibration phenomena at the points where the rotor speed was changed quickly. As shown in Fig. 7b, the phase current is about 4 (A) at lowest rotor speed (10 rad/s).

In the third simulation case, besides the changing of the desired rotor speed, the stator and rotor resistances are increased 1.5 times. In Figs. 8 and 9, the responses of the stator flux, load torque and rotor speed show that the performance of the SMC controllers are still stable. However, the phase current is about 3 (A) at lowest rotor speed (10 rad/s).

In order to verify the robustness of the proposed SMC controllers, in the fourth simulation case, the disturbances will be added in the simulation process. Figures 10 and 11 describe

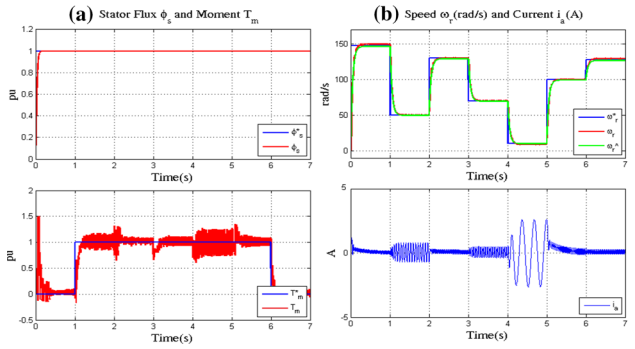

Fig. 9 The simulation results with case of changing the rotor speed and R_{r} is increased to 1.5 times. **a** The stator flux and torque T_{m}, **b** the rotor speed and phase current

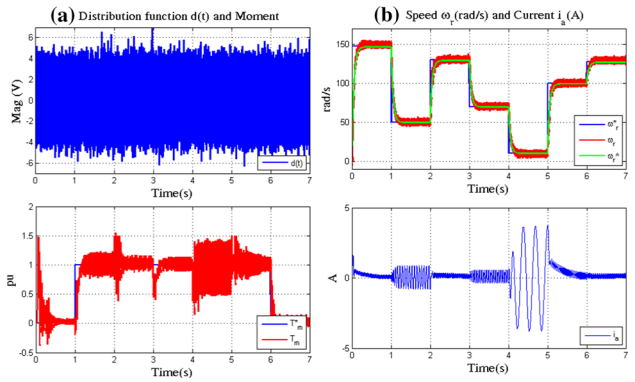

Fig. 10 The simulation results with case of adding the random distribution disturbances. **a** The disturbances and torque T_{m}, **b** The rotor speed and phase current

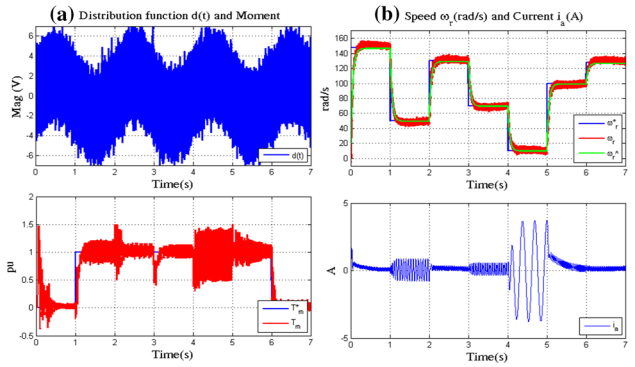

Fig. 11 The simulation results with case of adding the distribution disturbances typed sine wave. **a** The disturbances and torque T_{m}, **b** The rotor speed and phase current

the simulation results with the random and sine wave distribution disturbances, respectively. The disturbances have impact to the responses of the torque, stator flux and rotor speed. However, the tracking control for stator flux and rotor speed is still guaranteed. In addition, the phase current is also up to about 4 (A) at the lowest rotor speed (10 rad/s).

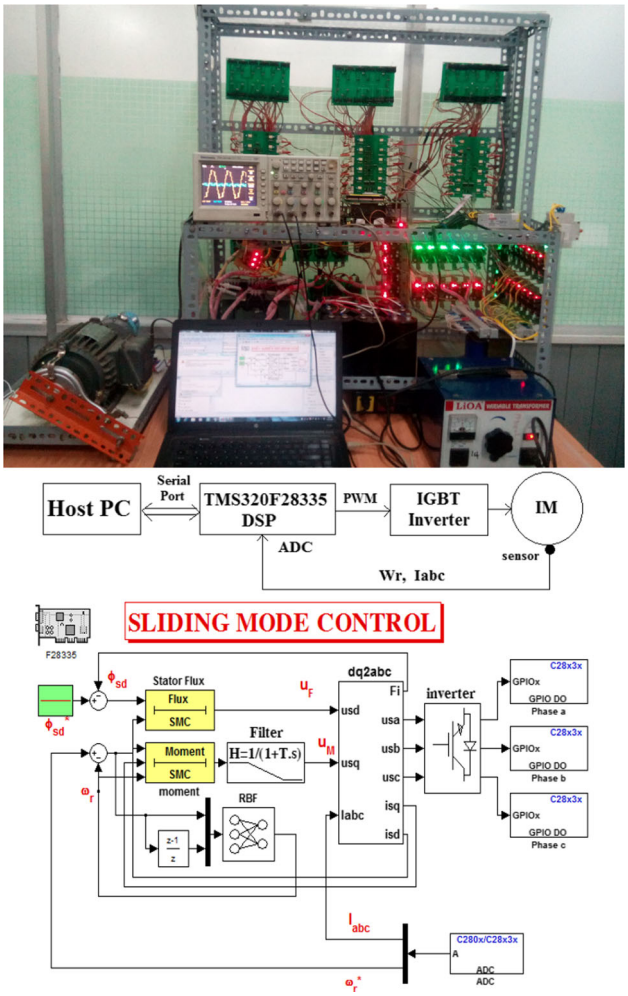

Fig. 12 The experimental TIM control system

Based on the simulation results, we easy realize that, with the proposed SMC controllers based on the NN estimator for the TIM 1 HP, 150 rad/s, the adaptive tracking control for the stator flux and rotor speed is well done. The NN estimator has played an important role in providing approximating rotor speed approximate with the rotor speed measured value. Moreover, for rotor speed tracking control, in considering the existence of the disturbances and the increasing of the resistances of stator/rotor (up to 1.5 times), the SMC controller-based NN has proven the robustness feature. This proposed control method cannot only guarantee the tracking control with the changing rotor speed, from lowest speed (10 rad/s) to highest speed (150 rad/s), but also guarantee the stability of phase current, the low CMV and THD.

4.2 Experimental results

Figure 12 shows the experimental TIM control system that is described briefly as follows. The designed SMC controllers-based NN estimator are embedded into the Digital Signal

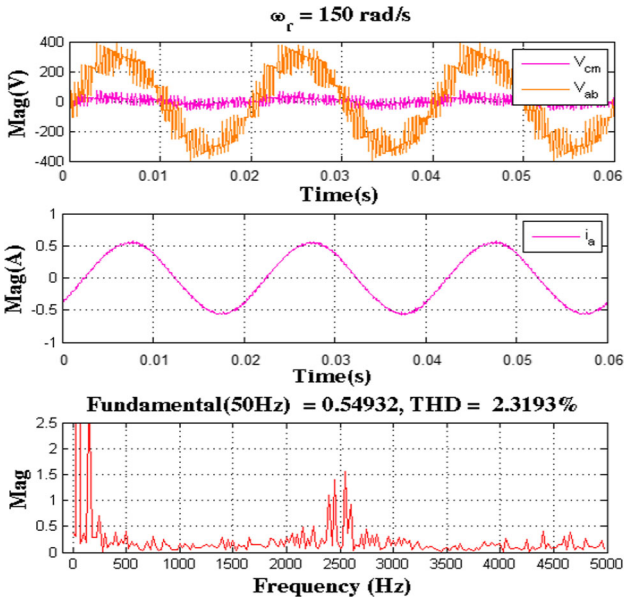

Fig. 13 The experimental results of the line voltage, CMV, phase current, THD and FFT of phase current (without the rated load)

Processing (DSP) 320F28355 card from Simulink/Matlab software (from host computer). The DSP card provide the control signals to control the TAIM via the IGBT inverter and receive the feedback signals from sensors (current, speed, stator flux and moment). The TIM system has technical parameters are same to the TIM model in the simulation process. We will test the effectiveness and robustness of the proposed control method with $\varphi_{sd}^{*} = 1$(Wb), $\omega_r^{*} = 150$(rad/s), and the TIM operate with and without the rated load.

Figures 13 and 14 present the experimental results of the line voltage, CMV, phase current, THD and FFT of phase current for the cases of no the rated load and adding the rated load, respectively. The CMV value is guaranteed with $V_{CM} = V_s/3$, the THD is low with THD $= 2.5 \rightarrow 4.062\%$, the phase current is about 4 (A). Figure 15 shows the experimental results of the stator flux and the moment. Based on these results (Fig. 15), the tracking control of stator flux is well done.

For the tracking control of rotor speed, we can observe based the results in Fig. 16. In Fig. 16a, without the rated load, the rotor speed track well to the desired rotor speed. In the other hand, in Fig. 16b, with the rated load, the tracking control for the rotor speed still guaranteed. However, with the rated load, the rotor speed fluctuates around the desired rotor speed. And this phenomenon shows that the proposed SMC controller based on NN estimator has proven the effectiveness and robustness characteristics. In addition, with and without the rated load, the NN estimator has updated itself and provided the rotor speed information. On the other hand, follow to the experimental result of the TIM torque, we can

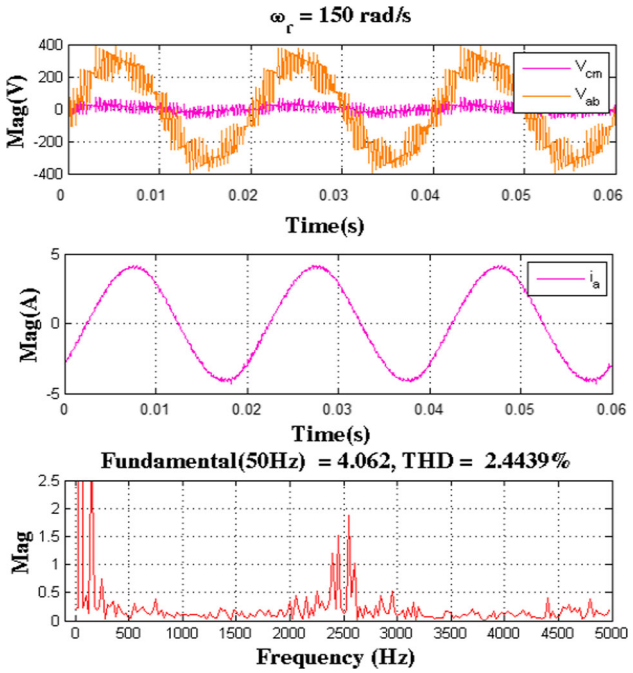

Fig. 14 The experimental results of the line voltage, CMV, phase current, THD and FFT of phase current (with the rated load)

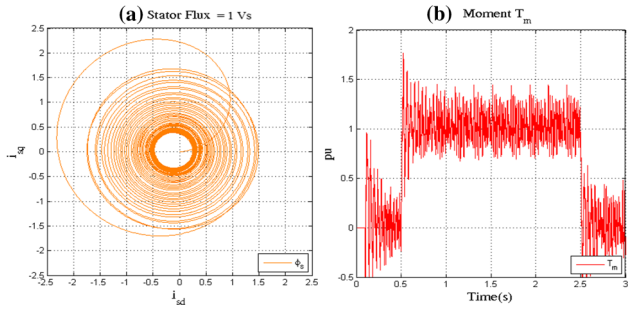

Fig. 15 The experimental results of the stator flux and moment T_m. **a** The stator flux, **b** the torque T_m

see that the SMC, with the tansig function for the switching surface, has limited the chattering phenomenon in the control process.

Based on the simulation and experimental results, we can confirm that the proposed SMC controllers based on the NN estimator has guaranteed well for the requirement of tracking control and robustness for the TIM control system.

5 Conclusions

The proposed method has successfully implemented the sensorless SMC scheme based on the NN for the TIM in the simulation and real-time practical. The NN estimator as the observer, has provided the rotor speed information for the control system without applying the sensors. By applying

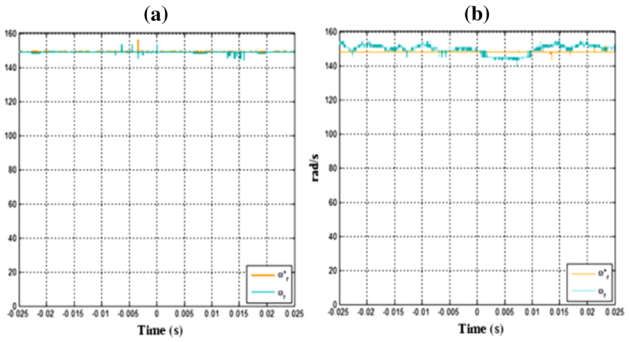

Fig. 16 The experimental results of the rotor speed. **a** Without the rated load, **b** with the rated load

the nonlinear function for the sliding switching surface, the proposed SMC method has guaranteed good performance for the chattering reducing and the tracking control of the stator flux and rotor speed. In addition, the stability and robustness of the proposed control system are also well done in the presence of disturbances and the changing of control parameters. The proposed sensorless SMC method based on the NN can be applied as a good alternative in the existing TIM control system.

Acknowledgements This work was supported by the Ho Chi Minh City University of Technology and Education and the Industrial University of Ho Chi Minh City, Vietnam. The authors would like to thank the associate editor and the reviewers for their valuable comments.

References

1. Guedes AS, Silva SM, Filho BJC, Conceicao CA (2016) Evaluation of electrical insulation in three-phase induction motors and classification of failures using neural networks. Elec Power Syst Res 140:263–273
2. Bouhoune K, Yazid K, Boucherit MS, Chériti A (2017) Hybrid control of the three-phase induction machine using artificial neural networks and fuzzy logic. Appl Soft Comp 55:289–301
3. Mamdouh M, Abido MA (2019) Efficient predictive torque control for induction motor drive. IEEE Trans Ind Electron 66(9):6757–6767
4. Accetta A, Alonge F, Cirrincione M, D'Ippolito F, Pucci M, Rabbeni R, Sferlazza A (2019) Robust control for high performance induction motor drives based on partial state-feedback linearization. IEEE Trans Ind Appli 55(1):490–503
5. Costa BLG, Graciola CL, Angelico BA, Goedtel A, Castoldi MF, Pereira WCA (2019) A practical framework for tuning DTC-SVM drive of three-phase induction motors. Control Eng Pract 88:119–127
6. Hajary A, Kianinezhad R, Seifossadat SG, Mortazavi SS, Saffarian A (2019) Detection and localization of open-phase fault in three-phase induction motor drives using second order rotational park transformation. IEEE Trans Power Electron 34(11):11241–11252
7. Shi S, Sun Y, Dan H et al (2020) A general closed-loop power-decoupling control for reduced-switch converter-fed IM drives. Electr Eng 102:2423–2433
8. Hung JY, Gao W, Hung JC (1993) Variable structure control: a survey. IEEE Trans Ind Electron 40(1):2–22

9. Utkin VI (1997) Variable structure systems with sliding modes. IEEE Trans Autom Cont 22(2):212–222
10. Bartolini G, Ferrara A, Usani E (1998) Chattering avoidance by second-order sliding mode control. IEEE Trans Autom Control 43(2):241–246
11. Lin F, Chang C, Huang P (2007) FPGA-based adaptive backstepping sliding-mode control for linear induction motor drive. IEEE Trans Power Electron 22(4):1222–1231
12. Ryvkin S, Schmidt-Obermoller R, Steimel A (2008) Sliding mode control technique for an induction motor drive supplied by a three-level voltage vource inverter. Facta Universitatis Ser Elec Energ 21(2):195–207
13. Yazdanpanah R, Soltani J, Arab Markadeh GR (2008) Nonlinear torque and stator flux controller for induction motor drive based on adaptive input–output feedback linearization and sliding mode control. Energy Convers Manag 49:541–550
14. Ahmed AHO, Ajangnay MO, Mohamed SA, Dunnigan MW (2010) Speed control of induction motor using new sliding mode control technique. In: 2010 1st international conference on energy, power and control (EPC-IQ), Basrah, 2010, pp. 111–115
15. Wai R, Chuang K, Lee J (2010) On-line supervisory control design for maglev transportation system via total sliding-mode approach and particle swarm optimization. IEEE Trans Autom Control 55(7):1544–1559
16. Oliveira JB, Araujo AD, Dias SM (2010) Controlling the speed of a three-phase induction motor using a simplified indirect adaptive sliding mode scheme. Cont Eng Pract 18:577–584
17. Kar BN, Choudhury S, Mohanty KB, Singh M (2011) Indirect vector control of induction motor using sliding-mode controller. In: International conference on sustainable energy and intelligent systems (SEISCON 2011), Chennai, 2011, pp. 507–511. https://doi.org/10.1049/cp.2011.0415
18. Fallaha CJ, Saad M, Kanaan HY, Al-Haddad K (2011) Sliding mode robot control with exponential reaching law. IEEE Trans Ind Electron 58(2):600–610
19. Zhang X, Sun L, Zhao K, Sun L (2013) Nonlinear speed control for pmsm system using sliding mode control and disturbance compensation techniques. IEEE Trans Power Electron 28(3):1358–1365
20. Qi L, Shi H (2013) Adaptive position tracking control of permanent magnet synchronous motor based on RBF fast terminal sliding mode control. Neurocomputing 115:23–30
21. Salih ZH, Gaeid KS, Saghafinia A (2015) Sliding mode control of induction motor with vector control in field weakening. Mod Appl Sci 9(2):276–288
22. Han SI, Lee JM (2015) Balancing and velocity control of a unicycle robot based on the dynamic model. IEEE Trans Ind Electron 62(1):405–413
23. Mohanty KB (2008) Sensorless sliding mode control of induction motor drives. In: TENCON 2008–2008 IEEE region 10 conference, Hyderabad. pp. 1–6. https://doi.org/10.1109/TENCON.2008.4766709
24. Veselic B, Perunicic-Drazenovic B, Milosavljevic Č (2010) Improved discrete-time sliding-mode position control using euler velocity estimation. IEEE Trans Ind Electron 57(11):3840–3847
25. Wang Y, Zhang X, Yuan X, Liu G (2011) Position-sensorless hybrid sliding-mode control of electric vehicles with brushless dc motor. IEEE Trans Veh Technol 60(2):421–432
26. Regaya CB, Zaafouri A, Chaari A (2014) A new sliding mode speed observer of electric motor drive based on fuzzy-logic. Acta Polytech Hung 11(3):219–232
27. Kommuri SK, Rath JJ, Veluvolu KC, Defoort M, Soh YC (2015) Decoupled current control and sensor fault detection with second-order sliding mode for induction motor. IET Cont Theo Appli 9(4):608–617
28. Hussain S, Abid-Bazaz M (2016) Neural network observer design for sensorless control of induction motor drive. IFAC-PapersOnLine 49(1):106–111
29. Boulghasoul Z, Kandoussi Z, Elbacha A et al (2020) Fuzzy improvement on Luenberger observer based induction motor parameters estimation for high performances sensorless drive. J Electr Eng Technol 15:2179–2197
30. Pimkumwong N, Wang M (2018) Full-order observer for direct torque control of induction motor based on constant V/F control technique. ISA Trans 73:189–200
31. Yin S et al (2020) Fast restarting of free-running induction motors under speed-sensorless vector control. IEEE Trans Ind Electron 67(7):6124–6134
32. Nikpayam M, Ghanbari M, Esmaeli A, Jannati M (2020) Fault-tolerant control of Y-connected three-phase induction motor drives without speed measurement. Measurement 149:1–14
33. Fu X, Li S (2015) A novel neural network vector control technique for induction motor drive. IEEE Trans Ener Conv 30(4):1428–1437
34. Kumar N, Chelliah TR, Srivastava SP (2015) Adaptive control schemes for improving dynamic performance of efficiency-optimized induction motor drives. ISA Trans 57:301–310
35. Lewis FL, Liu K, Yesildirek A (1996) Neural net robot controller with guaranteed tracking performance. IEEE Trans Neural Netw 6(3):703–713
36. Slotine JJE, Li W (1991) Applied nonlinear control. Prentice-Hall, Englewood Cliffs